On the Signal-to-Noise Ratio of MR-Based Electrical Properties Tomography

Seung-Kyun Lee[1], Selaka Bandara Bulumulla[1], and Ileana Hancu[1]
[1]*GE Global Research, Niskayuna, NY, United States*

Target Audience: Researchers interested in MR-based electrical properties measurement and mapping.

Introduction: MR-based electrical properties tomography (MREPT) computes relative permittivity (ϵ_r) and electrical conductivity (σ) from the Laplacian of the RF field map (e.g., B_1^+) in tissue [1,2]. In many cases the random noise in the input (B_1^+ map) is amplified by the Laplacian to limit the SNR of the calculated ϵ_r and σ. It is known experimentally that the SNR of MREPT rapidly degrades with decrease of the main magnetic field (B_0) [3], and is sensitive to the choice of the Laplacian calculation method. Here we analytically derive formulas for the SNR of MREPT that relate the input and the output noise in MREPT, and quantify the effect of B_0 strength and the region-of-interest (ROI) size on the SNR. SNR in phantom experiments is compared with the theory.

Theory: *MREPT equations.* We start with the MREPT equations Eqs. (1,2). Numerical computation of $\nabla^2 B_1^+$ involves multiple voxels in a region centered at a voxel of interest; we will call such a region an ROI. For a given ROI, most published methods to compute $\nabla^2 B_1^+$ from B_1^+— such as the integral method, difference equation, and least-squares polynomial fitting — are linear in B_1^+ and can be generalized as $\nabla^2 B_1^+ = \sum_{v\in ROI} B_{1,v}^+ \cdot g_v \equiv \langle B_1^+ \rangle_g$, where g_v is a real-valued, linear Laplacian kernel. Using this, we rewrite Eqs. (1,2) as Eqs. (3,4), where we also replaced B_1^+ by its "estimator" in the ROI, $\langle B_1^+ \rangle$. Exact definition of $\langle B_1^+ \rangle$ is unimportant; e.g., it can be an average of B_1^+ in the ROI. Next, we define auxiliary variables b_r and b_i, Eqs. (5,6), which are the real and imaginary parts of the B_1^+ map scaled by $\langle B_1^+ \rangle$. Eqs. (3,4) are then equivalent to Eqs. (7,8).

$$\epsilon_r = -\frac{1}{\omega^2 \epsilon_0 \mu_0} Re\left(\frac{\nabla^2 B_1^+}{B_1^+}\right) \quad (1)$$

$$\sigma = \frac{1}{\omega \mu_0} Im\left(\frac{\nabla^2 B_1^+}{B_1^+}\right) \quad (2)$$

$$\epsilon_r = -\frac{1}{\omega^2 \epsilon_0 \mu_0} Re\left(\frac{\langle B_1^+ \rangle_g}{\langle B_1^+ \rangle}\right) \quad (3)$$

$$\sigma = \frac{1}{\omega \mu_0} Im\left(\frac{\langle B_1^+ \rangle_g}{\langle B_1^+ \rangle}\right) \quad (4)$$

$$b_r \equiv Re\left(\frac{B_1^+}{\langle B_1^+ \rangle}\right) \quad (5)$$

$$b_i \equiv Im\left(\frac{B_1^+}{\langle B_1^+ \rangle}\right) \quad (6)$$

$$\epsilon_r = -\frac{1}{\omega^2 \epsilon_0 \mu_0} \langle b_r \rangle_g \quad (7)$$

$$\sigma = \frac{1}{\omega \mu_0} \langle b_i \rangle_g \quad (8)$$

Noise. We assume that $|B_1^+|$ and $\angle B_1^+$ maps are separately acquired so their noise is independent. Furthermore, each voxel has a statistically independent and voxel-independent amplitude noise $\Delta|B_1^+|$ and phase noise $\Delta\angle B_1^+$; the symbol Δ denotes statistical uncertainty. The SNR of B_1^+ is defined as $SNR_{|B_1^+|} \equiv \overline{|\langle B_1^+ \rangle|}/\Delta|B_1^+|$, $SNR_{\angle B_1^+} \equiv 1/(\Delta \angle B_1^+)$; here the bar ($\bar{}$) denotes a statistical expectation value. The noise in b_r and b_i can be approximated by Eqs. (9,10) under the following realistic conditions: (i) true spatial variation of B_1^+ in the ROI is weak compared to $\overline{|\langle B_1^+ \rangle|}$, and (ii) $\langle B_1^+ \rangle$ has lower statistical uncertainty (because it is averaged over many voxels) than B_1^+ of individual voxels. Eqs. (11,12) express the fact that statistical uncertainty of the weighted sum of a variable (b_r or b_i) equals that of the variable itself times the root sum of squares (rss) of the weighting function (g).

$$\Delta b_r \approx \frac{1}{SNR_{|B_1^+|}} \quad (9)$$

$$\Delta b_i \approx \frac{1}{SNR_{\angle B_1^+}} \quad (10)$$

$$\Delta\langle b_r \rangle_g = \Delta b_r \cdot rss(g) \quad (11)$$

$$\Delta\langle b_i \rangle_g = \Delta b_i \cdot rss(g) \quad (12)$$

$$rss(g) = \frac{G}{N_{tot}^{1/2} L^2} \quad (13)$$

$$\Delta\epsilon_r = \frac{1}{\omega^2 \epsilon_0 \mu_0} \cdot \Delta\langle b_r \rangle_g \quad (14)$$

$$\Delta\sigma = \frac{1}{\omega \mu_0} \cdot \Delta\langle b_i \rangle_g. \quad (15)$$

$$SNR_{\epsilon_r} \equiv \epsilon_r/\Delta\epsilon_r = SNR_{|B_1^+|} \cdot \sqrt{N_{tot}} \cdot \omega^2 \epsilon_0 \epsilon_r \mu_0 \cdot L^2/G \quad (16)$$

$$SNR_{\sigma} \equiv \sigma/\Delta\sigma = SNR_{\angle B_1^+} \cdot \sqrt{N_{tot}} \cdot \omega\sigma\mu_0 \cdot L^2/G \quad (17)$$

Minimum-noise Laplacian kernel. It can be shown that among all linear Laplacian kernels, the one based on the Savitzky-Golay filter has the lowest rss value [4]. For such a kernel, the rss is given by Eq. (13), where N_{tot} is the number of voxels in the ROI, L is ROI's linear dimension, and G is a factor that depends on the ROI shape; a disc with diameter L has $G_{disc} = 32\sqrt{3}$ and a sphere with diameter L has $G_{sphere} = 20\sqrt{21}$. Finally, the noise in ϵ_r and σ can be obtained from Eqs. (7,8) as Eqs. (14,15). Substituting Eqs. (11-13) to Eqs. (14,15), followed by substitution of Eqs. (9,10) leads to our main results, Eqs. (16,17).

Methods and Results: Three cylinders filled with salt water with different concentrations were scanned in a GE Discovery 3.0 T MR750 scanner for $|B_1^+|$ (Bloch-Siegert) and $\angle B_1^+$ (1/2 spin echo phase) maps in an axial orientation. The diameter of cylinders was 85 mm. Dielectric probe measurements yielded reference σ = 0.45, 1.11, 1.76 [S/m] for the three cylinders, and reference ϵ_r = 74 was estimated by low-noise MREPT reconstruction. The $|B_1^+|$, $\angle B_1^+$ map scans were repeated 15 times. Each time ϵ_r and σ were computed at the center of the cylinder in a 2D circular ROI of varying diameters, L = 6~30 mm; slice-direction variation of B_1^+ was ignored due to axi-symmetric geometry. A Laplacian kernel based on the Savitzky-Golay filter was used for reconstruction. Standard deviation of ϵ_r and σ over the 15 measurements and the reference values were used to compute the MREPT SNR, to be compared with predictions of Eqs. (16,17) with $G = G_{disc}$. Experimental and theoretical SNR agreed reasonably well for small ROI, up to about L = 12 mm (Fig. 1). For larger ROI, measured SNR was generally lower than theory.

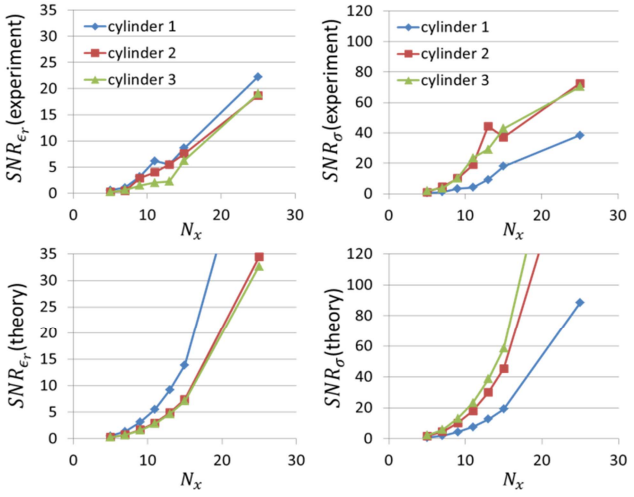

Figure 1. Experimental (top) vs theoretical (bottom) SNR in MREPT as a function of the ROI diameter in pixels (= N_x, 1 pixel = 1.17 mm). Cylinders 1,2,3 had σ = 0.45, 1.11, 1.76 S/m, respectively. Error bar in the experimental SNR, due to finite (15) sample size, is about ±20% [6].

Discussion: Rapid initial increase of measured SNR in ϵ_r and σ with the ROI size was correctly predicted by our theory. Failure of continued fast rise in SNR can be attributed to spatially correlated noise in measured B_1^+ maps, analogous to scanner-dependent correlated noise in fMRI data [5]. Eqs. (16,17) also predict how MREPT SNR depends on B_0 (through ω). Rapid rise of SNR_{ϵ_r} with B_0 agrees with ref. [3]. Our results can provide a guide for experimental design in MREPT by quantifying the random noise-limited SNR in MREPT.

This work was supported by the NIH grant 1R01CA154433. The views herein do not necessarily represent those of the NIH. **References:** [1] Haacke et al., Phys Med Biol 36:723-734 (1991). [2] Katscher et al., Comput Math Methods Med 2013: 546562. [3] van Lier et al., MRM 71:354-363 (2014). [4] Lee S-K., ISMRM 2015 (submitted). [5] Friedman et al., JMRI 23:827-839 (2006). [6] Ahn S. et al., http://web.eecs.umich.edu/~fessler/papers/files/tr/stderr.pdf